ISBN: 978-981-18-5852-9
WCSE 2022 Spring Event: 2022 9th International Conference on Industrial Engineering and Applications
doi: 10.18178/wcse.2022.04.101

Development of a 3D Printed Origami Robotic Arm Inspired by Elephant Trunk

Yi-Shi Xie [1], Yanwen Han [1] and Ki-Young Song [1 +]

[1] School of Mechatronical Engineering, Beijing Institute of Technology

Abstract. In this research, we propose a new design and fabrication process of a soft robotic arm based on 3D printed origami with thermoplastic polyurethane (TPU), and the mechanism of the robotic motion is inspired by an elephant trunk. An optimized intricate design of the 3D printed origami successfully reproduces the folding function of conventional paper-based origami. A transform motion of the 3D printed soft physique is influenced by the structural dimension and the reacting forces to form the final configuration. Stacking multiple modules of the 3D printed soft origami, a soft robotic arm is built, and the robotic arm is controlled by wires to perform movements of an elephant trunk. Our proposed soft robotic arm is lighter and more flexible with high degrees of freedom and shrinking. Additionally, the proposed soft robotic arm can perform convoluted postures and operate tasks, such as manipulation of objects.

Keywords. 3D print, origami, module, robotic arm, wire control

1. Introduction

A robotic arm is one of the most popular and fast developing research topics in recent years. It has been applied in various areas such as industry, medical, aerospace, and so on. Though robotic arms have been dominantly made of hard material, recent studies in soft robots have demonstrated the advantage and the potential of soft robots. Especially in medical fields, the inherent characteristics of soft material have provided robots immutable advantage over traditional hard materials [1].

Soft robotic arms are usually in the shape of snakes or caterpillars. With proper maneuver scheme, they can function or behave like an elephant trunk or an octopus's tentacles. The structure of a soft robotic arm is designed to have plenty of degrees of freedom (DoFs). A high DoF provides an outstanding flexibility as well as a super compliant body that can withstand shock or sudden forces, which avails the soft robots' adoption in protecting objects they interact with.

One specific category of soft robotic arm is origami robotic arm. Origami robotic arms usually achieve their function through folding. In various designs, an origami robot arm can balance rigidity and flexibility to a fine point, depending upon applications. Many researches have adapted Kresling origami to build similar structures [2-4] which are capable of performing both rotational and prismatic movement. By connecting multiple segments of a modular structure into a longer arm, operations of the connected body are amplified. Thus, a robotic arm can be applied in many practical usages. Santoso and Onal [5] proposed another origami-based structure, using strings for motion control. They successfully achieved a high precision control of the origami robotic arm. Although numerous origami-based soft robotic arms have been developed, the fabrication of the robotic arms has been limited with folding sheets of papers and polymers.

This paper introduces a new approach of 3D printable origami-based soft robotic arm inspired by an elephant trunk. Instead of using sheets of papers like most origami robotic arms, we adapt 3D print with thermoplastic polyurethanes (TPU) to fabricate a functional soft robotic arm. Compared to other origami robotic arms, our design and fabrication approach has advantages of better durability, better resilience, and easy fabrication, and the structure is highly modular. Our proposed structure design adapts "bendy straws" designed by Evandro Bernardes who introduced mathematical models of origami designs and prototypes of

+ Corresponding author. Tel.: +8617812160115.
E-mail address: kiyoungsong@bit.edu.cn

paper origamis [6]. The proposed design is adequate for various manipulations with retracting in great distance and tilting in all directions.

2. Material and Method

2.1. Material

In this study, all the structure parts were fabricated by a commercial fused deposition modeling (FDM) 3D printer (ANYCUBIC Mega-S, China) with a nozzle diameter of 0.4 mm. A TPU 85A filament of 1.75 mm (Attoblue, China) was purchased for 3D printing. The density of the filament is around 1.2 g/cm^3 and its Young's modulus is between 10-12 Mpa [7]. Those characteristics of the filament sufficed properties for an origami robotic arm.

2.2. Mathmatical Principles and Structure Design

For the design of the origami structure, we studied and modified the "bendy straws". As shown in Fig. 1, the red and blue lines on the planar design represent valley creases and mountain creases, respectively. Combined together, they form an outside reverse fold. Those repeated patterns were capable of generating 3D folding structures with a specific angle.

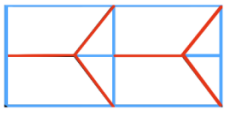

Fig. 1 The basic pattern of origami for the proposed soft robot arm.

The folding process of a single half pattern is illustrated in Fig. 2. When the green triangle folds to the red trapezoid, the blue rectangle rotates and covers the green area, forming an angle of:

$$\alpha = 180° - 2\beta \tag{1}$$

If this angle α is exactly equal to the inner angle of an equilateral polygon of n sides, then we can combine n identical patterns in a way that red areas connect to blue areas to make a ring of n sides. Then, the structure composes a sleeve of n faces in natural state and a flattened ring of n sides when folded.

One important aspect of this pattern is that in this geometry model, the red and blue areas (faces) in Fig. 2 should be rigid to keep their initial shapes during the folding. In another word, the mechanism of folding such a structure does not require bending or deformation of those rigid faces (in red and blue). The folding process is only accomplished by rotating the rigid faces about a specific axis. Thus, no interference should happen during transformation in theory.

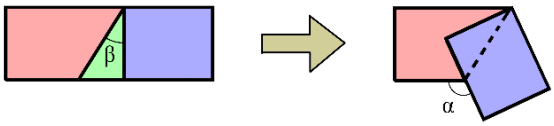

Fig. 2 The folding mechanism of outside reverse fold.

In this origami design, we used β = 30°; thus, the angle α after folding became 120°. By connecting 6 consecutive patterns head-to-tail, the origami was capable to be folded into a hexagon-shaped-ring. From our observation, the hexagon exhibited an easier motion control and larger contact area when interacting with other objects.

2.3. Fabrication

To realize the functions of patterns in reality with 3D printing, we firstly used SOLIDWORKS to create a 3D model of an origami sheet for folding and a link for constraining the movement of origami.

For origami sheet, we designed the pattern to better fit the characteristic of TPU. As shown in Fig. 3 (a), the green area is a thin film, and the blue areas are plates attached on the film. By the difference of thickness between plates and films as shown in the figure, the stresses on the sheet was redistributed in a desired way for a proper folding. Each sheet contains six identical patterns, and the length and the width of an origami sheet was 114 mm and 20 mm, respectively. The thickness of the sheet was varied by the plate thickness *H* and the film thickness *h* (Fig. 3 (b)), and the effect of the thickness on the structural performance was investigated by experiment.

We designed a hexagon-shaped link to attach on the origami sheet as shown in Fig. 3 (c), and protuberances were added with holes at each corner of the hexagon. The protuberant holes provided the path of wires to control the folding of the origami modules.

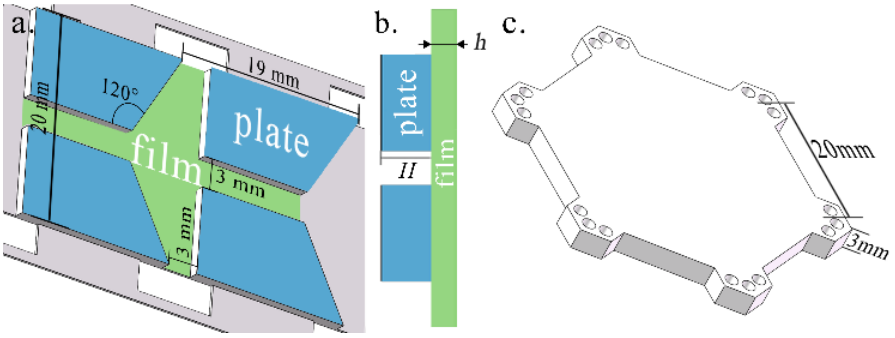

Fig. 3 (a) The modified pattern for TPU 85A and its parameters (b) The thickness parameters of origami sheets (c) Link parts and its parameters

The origami module was 3D printed with TPU 85A filament which required a distinct printing setting as listed in Table 1.

Table 1: Key parameters of the printing setting

Parameters	Value
Nozzle Temperature	225℃
Bed Temperature	50℃
Layer Height	0.1 mm
Line Width	0.4 mm
Infill Density	150%
Print Speed	25 mm/s

Additionally, printing the demanded model needed special adjustment of the bed height to satisfy the film thickness of 0.1 mm due to the higher infill density which made the printed structure tighter without void area between printed filament strings. We found that a closer distance (< 100 μm) between the printer nozzle and the printing bed was necessary to achieve a better quality of the demanded printing.

After printing the origami sheet and the link, we wrapped the sheet into a sleeve and glued the head and the tail together. Then, we assemble the link onto the sleeve using the alignment holes designed on the film to get a completed origami module as shown in Fig. 4.

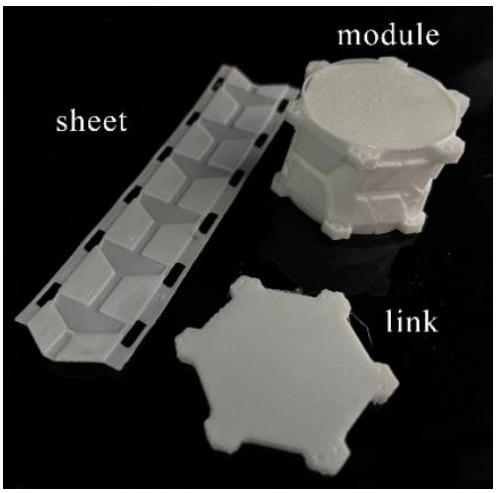

Fig. 4 Completed origami module and its components.

3. Experiments

With the planar parameters fixed, we study how different plate thickness *H* and film thickness *h* affect the force reaction of one origami module

We first investigated the reaction force by the origami module with the characteristic curve as shown in Fig. 5. Using a digital force gauge (DS2-500N, China), we compressed a module and measured the reaction force at every 0.5 mm displacement. Since the tension within the structure dissipated slower in soft materials, we waited 10 seconds and recorded the data at every displacement. We noticed that the force firstly surged up to a certain level at only a small compression and then fell down as the compression grew larger. Eventually, the force increased boundlessly as the total displacement was close to the height of an origami segment.

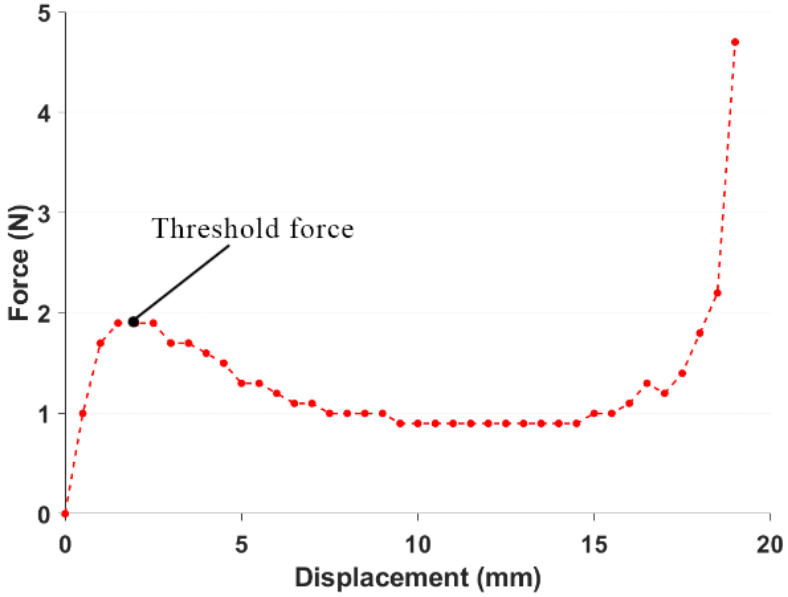

Fig. 5 The characteristic curve of the origami reaction force

We believed that the peak force at the early stage of the folding conducted the formation as a threshold force. Only when the force was larger than the threshold force, the folding process could be actuated and finished. The threshold force was obviously related to the thickness of origami sheets. Thus, we investigated a variety of different *H*s and *h*s for the experiment.

3.1. The Range of Variables

For the range and value of *H*, we selected three different values: 0.5 mm, 1.0 mm and 1.5 mm. From the observation, we found that when $H < 0.5$ mm, the plates were easily bend and deform, which caused failures of folding by concentrating the stress to the designed area. When $H > 1.5$ mm, the space between two plates was too small, leading a unwanted interference of plates with higher reacting force.

For the range and value of *h*, we also selected three different values: 0.3 mm, 0.4 mm, 0.5 mm. By the limitation of the 3D printer we used, a film with $h < 0.3$ mm was not achievable. From our observation, films with $h > 0.5$ mm was difficult to be properly folded.

3.2. The Experiment procedure

Matching different *H* and *h*, we got 9 different designs as listed in Table 2. We printed 3 samples for each design and measured the reaction force with the force gauge by compressing the sample until the force reached a peak (threshold force) by 0.5 mm displacement.

Table 2. The threshold force

Parameter Setting		Threshold Force	
h (mm)	H (mm)	Mean	STD
0.3	0.5	2.27	0.32
	1.0	3.10	0.93
	1.5	2.20	0.61
0.4	0.5	6.03	0.47
	1.0	6.90	0.70
	1.5	6.26	0.55
0.5	0.5	10.73	1.02
	1.0	7.67	0.38
	1.5	9.97	0.87

First, the film thickness *h* was a major factor of deciding the threshold force. Increasing the film thickness by 0.1 mm lead to an increase of approximately 3 N threshold force. The result fit our anticipation that thicker films would be stiffer than thinner ones.

Second, the plate thickness *H* worked in a more complicated way. It was observed that as *H* increased from 0.5 mm to 1.0 mm, the threshold force also increased. However, as *H* increased from 1.0 mm to 1.5 mm, the threshold force decreased instead. From the observation, we assumed that thicker plates induced the film folding. Thicker plates (from 1.0 mm to 1.5 mm) became too stiff to be deformed, which caused more stress and tension concentrated on the film; thus, the film was taking more stress to be folded. The mechanism abovementioned was more apparent with 2.0 mm plates which had smaller threshold force (not listed in the table) from our experiment.

At $h = 0.5$, the reaction force was inversely proportional to *H* different from cases of thinner films. We assumed that the ratio of *h* to *H* affected the threshold force. We found that the threshold forces occurred at $h/H = \sim 0.5$ which was the ratio for the smallest threshold force at $h = 0.5$ mm and $H = 1.0$ mm. We also assumed that the threshold force again increased as the ratio (h/H) was higher than ~0.5 which was indicated in the case of h $H = 1.5$ mm. At $H = 0.5$ mm, we found that the ratio (h/H) was too low for the plates to successfully concentrate the stress onto the films. Thus, the threshold force was relatively higher, which caused frequent failure of proper folding procedure. When the origami was folded improperly, the threshold force was significantly larger.

3.3. Robotic Arm

With various design parameters, we achieved different threshold forces to build a robotic arm and to control the arm with wires, mimicking an elephant trunk.

From the results, we selected 3 different designs, h = 0.3 mm and H = 0.5 mm, h = 0.4 mm and H = 1.5 mm, and h = 0.5 mm and H = 1.5 mm, corresponding to upper, middle, and lower sections of the robotic arm, respectively. The selection allowed different acting force for bending.

Each section was consisted of three identical origami segments, and was controlled by three finishing wires spacing 120° at corners of links. The protuberant corners with holes on the links held wires in position. By pulling wires, each section of the arm bent to any direction or was simply contracted.

The design of the robotic arm admitted different applying forces for bending at different sections: The upper part needed the smallest threshold force, and the lower part required the biggest threshold force; thus, when one section of the robotic arm bent, the section minimally affected the other sections beneath. Based on this arrangement and mechanism, we achieved independent control of all sections of the soft robotic arm.

3.4. Performance

We tested the performance of our origami robotic arm through various ways.

First, we calculated the theoretical maximum bending angle of the structure at six corners as

$$\theta_{\max} = n\cos^{-1}(1-\frac{l_1^{\,2}}{2(d_1+d_2)^2}) \tag{2}$$

where n is the number of origami segments; l_1 is the height of one origami segment; d_1 is the diameter of hexagon links; d_2 is the length of the protuberance on the links. In our design, n = 9, $l_1 = 20mm$, $d_1 =$ 40mm, $d_2 = 1.5\ mm$, and we got an estimated $\theta_{max} = 251.0°$.

Then, we tested the bending of the robotic arm in reality to compare the actual bending angle at each direction as illustrated in Fig. 6.

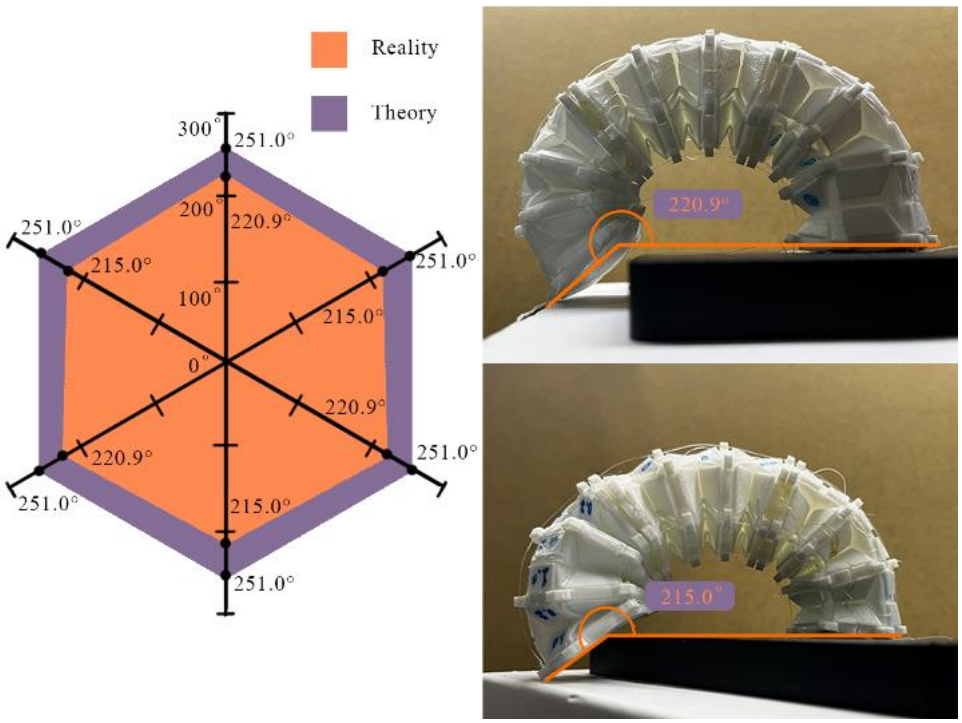

Fig. 6 The maximum bending angle of the arm at different direction.

From the result, we observed that the real maximum bending was less than the estimation. It was because links were slightly deformed by absorbing acting forces for bending from the wires, and some friction occurred between wires and holes which also negatively affected the manipulation during bending.

Next, we drove the robotic arm for different posture as shown in Fig. 7. The arm had a total of nine wires, and each wire pulled a section to be bent to a direction. Combining different wires, the arm was able to fully contract single section, to partially bend, and to form an “S” shape. By proper maneuver, the arm was also capable of picking up a small object and hold it by wrapping.

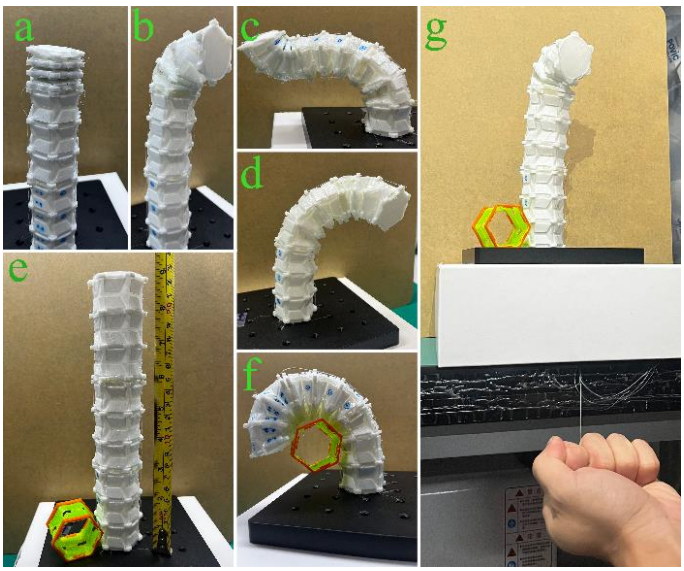

Fig. 7 Manipulation of the origami robotic arm and various postures: (a) contract single section; (b) partially bend; (c) form an “S” shape; (d) twist self; (e) stand straight; (f) hold an object; (g) maneuver by pulling wires.

4. Conclusion

In this study, a new type of origami soft robotic arm was introduced, inspired by an elephant trunk. The soft robotic arm was composed of multiple soft origami modules and was successfully manipulated by wires with high degrees of freedom for bending, posturing, and holding. The module was fabricated by conventional 3D printing process with TPU material. The origami module was consisted of a film and plates in various thicknesses, and the thickness were analyzed to explore reaction forces to discover threshold forces which initiated a folding of the module. We found that film thickness was the major determinant of the reaction force, and the plate thickness was crucial to ensure a proper folding of origami. Combining the soft origami modules with different threshold forces, we were able to build an origami robotic arm with high flexibility. Furthermore, different sections of the robotic arm were individually controlled by wire control. We manipulated the origami robotic arm into various postures and managed the arm to complete simple tasks, picking up an object and holding it. The results declare the flexibility of this soft origami robotic arm and support the potential functioning of this arm as a versatile soft manipulator.

5. Acknowledgment

This work was supported by grants from Beijing Institute of Technology Research Fund Program for Young Scholars (grant number 3020012222017).

6. References

[1] H. J. Chung, A. M. Parsons, and L. Zheng, “Magnetically controlled soft robotics utilizing elastomers and gels in actuation: a review”, Adv. Intell. Syst., vol. 3, 2000186, 2021.

[2] L. Mena, J. Muñoz, C. A. Monje, and C. Balaguer, “Modular and Self-Scalable Origami Robot: A First Approach”. Mathematics, vol. 9, 1324, 2021.

[3] S. Wua, Q. Zea, J. Daia, N. Udipib, G. H. Paulinob, and R. Zhaoa, “Stretchable origami robotic arm with omnidirectional bending and twisting”, Proceedings of the National Academy of Sciences, Vol. 118, 2021.

[4] P. Bhovad, J. Kaufmann, and S. Li. “Peristaltic locomotion without digital controllers: Exploiting multi-stability in origami to coordinate robotic motion”, Extreme Mechanics Letters, Vol. 32, 100552, 2019.

[5] J. Santoso and C. D. Onal. “An origami continuum robot capable of precise motion through torsionally ttiff body and smooth inverse kinematics”, Soft Robotics Vol. 8, pp. 371-386, 2020.

[6] E. Bernardes and S. Viollet, “Design of an origami bendy straw for robotic multistable structures”, Journal of

Mechanical Design, Vol. 144, 033301, 2021.

[7] H. Mi and X. Jing. “Approach to fabricating thermoplastic polyurethane blends and foams with tunable properties by twin-screw extrusion and microcellular injection molding”, Adv Polym Technol, 33, 21380, 2014